How to design a zero-degradation battery: compensating for loss of lithium inventory in LFP cells with LFO additives

Sunil Kumar Rawat*, Monica Marinescu, Gregory James Offer, Simon E. J. O'Kane, Ruihe Li

*Corresponding author:
E-mail address: s.rawat@imperial.ac.uk

Affiliations:
Department of Mechanical Engineering,
Electrochemical Science and Engineering Group
Imperial College London

Abstract

Controlling lithium-ion battery degradation is a major global challenge and essential to electrify transport, deploy storage on the grid, and extend the lifetime of portable electronics. Loss of lithium inventory (LLI) caused by side reactions in lithium-ion cells is one of the primary reasons behind their shorter cycle life. Researchers in the last ~15 years have demonstrated that additives such as Lithium Iron oxide Li_5FeO_4 (LFO) in LFP-based chemistries can irreversibly release their lithium to compensate for LLI. More recently, CATL and Rimac have commercialised LFO in LFP cells, claiming to have achieved zero degradation for extended periods. However, the specifics of how they achieved this are neither fully disclosed by them nor much explored in the literature.

This work describes how LFO can be employed in commercial LFP cells using a full-cell physics-based model in PyBaMM to achieve so-called 'zero degradation'. We first attempt to find the optimal methods to control lithium release from LFO by simulating 2000 charge/discharge aging cycles for five cases to investigate how controlled lithium release speed (slow or fast release) and timing (early or later part of cell life) can impact cell degradation and its life. We then use the model to find an optimum weight fraction of LFO that can be used in LFP cells to maximize cell life. Model results reveal that slow lithium release maintains the cell balancing and reduces the cell degradation rates. In contrast, rapid lithium release and excessive LFO content can accelerate cell degradation rates resulting in lower cycle life. The results also reveal that the large anode overhang can help prevent cell unbalancing however it presents a trade-off between achieving higher cycle life and maintaining energy density. The model assumes that oxygen released during LFO delithiation can be managed by cell degassing and advanced cathode coating agents and hence doesn't affect cell degradation. This work shows that achieving longer cell life requires not merely adding lithium-rich additives like LFO but also the ability to control the lithium and oxygen release through appropriate methods.

Main

Loss of lithium inventory (LLI) is one of the major consequences of degradation and the reasons behind capacity fade and reduced life cycle in lithium-ion batteries (Birkl et al., 2017), (Edge et al., 2021). The formation of the solid electrolyte interphase (SEI) along with other degradation

mechanisms in lithium-ion cells leads to the consumption of lithium ions and hence LLI (Edge et al., 2021). LLI is particularly intense during formation and potentially during the first few cycles of operation because of the initial formation of the SEI. Recent breakthroughs in research and industry have explored how LLI can be compensated by using an additive that can release additional lithium inventory in a controlled way, thus improving battery longevity. Lithium iron oxide Li_5FeO_4 (LFO) is seen as an excellent candidate for its use as an additive for lithium iron phosphate (LFP)-based battery chemistries (Johnson et al., 2010), (Su et al., 2016), (Liu et al., 2024). The antifluorite structure of LFO active material helps it to store as much as four times (per gram) more lithium ions (Johnson et al., 2010) compared to LFP active material, helping it to achieve significantly higher theoretical and practical capacity per gram (Dose et al., 2018) (Liu et al., 2024). The stored lithium ions in LFO are released permanently in two stages at open circuit potentials vs. lithium (OCP) of 3.5 V and 4.0 V when the cell is overcharged (Johnson et al., 2010), (Liu et al., 2024), making it traditionally suitable only for primary cells. In a secondary cell, the lithium released has been used to compensate for LLI (Johnson et al., 2010), (Su et al., 2016), (Dose et al., 2018), (Liu et al., 2024). The use of LFO as a sacrificial agent in the lab scale cells showed that LFO can successfully compensate for LLI during formation and subsequent charge-discharge cycles and help maintain stable cell performance. Companies such as CATL and Rimac have demonstrated the commercial viability of LFO being used in this way (Pathirana, 2024), (Murray, 2024). CATL showed that LFO can be implemented as a cathode additive in LFP batteries to achieve zero apparent degradation for the first 1000 cycles (Pathirana, 2024). They focused on lithium release from LFO in the early phase of the battery's life. Rimac Energy's approach is slightly different as they hint towards gradual lithium release from LFO and claimed to have achieved zero capacity fade for two years (Murray, 2024). Rimac has also mentioned using an advanced power conversion system to achieve such performance (Murray, 2024). Neither of the two companies has disclosed the exact methods, leaving researchers to speculate about the underlying principles, mechanisms, and methods of successfully employing LFO as an additive in commercial cells. Commercial-level use of LFO and the understanding of how to use it are also missing in the literature. Using the above innovations as motivation, our work offers a detailed insight into how LFO can be employed in commercial LFP cells with LFP/LFO positive electrode (PE) and Graphite negative electrode (NE) using simulations run by building a full-cell physics-based model in PyBaMM and analysing its predictions.

This work adds to our understanding of the science and the consequences of releasing additional lithium from LFO, its impact on cell degradation (SEI, lithium plating, porosity clogging), discharge capacity, and cell life. The degradation consequences are not always beneficial, therefore the work attempts to find the optimal methods to control lithium release from LFO, an optimum weight fraction of LFO, and explores the possibility of using larger NE overhang to minimize cell degradation and achieve long-lasting, zero-degradation batteries using the model predictions. The first two sections discuss the mechanism of lithium and oxygen release and their relationship with cell charging voltage. Afterward, the impact of released lithium from LFO on degradation, cell capacity, and cell life is discussed in the next two sections. Then a detailed analysis of various control methods for optimal lithium and oxygen release and optimal weight fraction of LFO to be used in LFP-LFO cells for achieving maximum cell performance can be found. The methods section discusses the model implementation, model setup, assumptions, virtual experiments set up in PyBaMM, and the PyBaMM setup of methods of controlled lithium release from LFO. The conclusion section summarises the main results of this work and its impact.

Understanding the theoretical mechanism of lithium and oxygen release from LFO

LFO (Li_5FeO_4) material as a sacrificing agent in lithium-ion cells releases its lithium inventory by following the below two reactions:

$$Li_5FeO_4 \rightarrow Li_3FeO_{3.5} + 0.25O_2\uparrow + 2Li^+ + 2e^- \quad [1]$$

$$Li_3FeO_{3.5} \rightarrow LiFeO_2 + 0.75O_2\uparrow + 2Li^+ + 2e^- \quad [2]$$

The first irreversible release of lithium-ions happens when the half-cell open-circuit potential (OCP) of LFO is between 3.5 V and ~3.75 V (reaction [1]) and the second irreversible lithium release happens when the OCP is between ~3.75 V and 4.5 V (reaction [2]) (Liu et al., 2024). Figure 1 shows the half-cell OCP of a pure LFO material (Liu et al., 2024) vs stoichiometry. The two relative plateaus at ~3.5 V and ~4.0 V correspond to the two stages of lithium release from LFO. We define the stoichiometry of fully lithiated LFO as 1 (i.e. Li_5FeO_4) with an OCP of 3.5 V and the stoichiometry of depleted LFO as 0 (i.e. $LiFeO_2$) with an OCP of 4.5 V. As the LFO releases its lithium irreversibly, if the positive electrode potential drops below the OCP of LFO then nothing happens, until the potential increases again, hence the stoichiometry will always decrease monotonically from 1 to 0. Considering the equations above it is worth noting that some oxygen is also released from the LFO when it releases its lithium. This is rarely discussed in the literature on LFO but is known to contribute to different degradation mechanisms. In this work, we neglected the oxygen-related degradation because we assume that most oxygen released from LFO is removed by performing cell degassing during the initial few cycles. The remaining negligible fraction of oxygen, which is released during the later part of cell life, can be captured through the suitable oxide and phosphate coatings on the cathode surface and hence doesn't affect cell degradation. It is worth noting that the moles of oxygen released depend upon the initial LFO moles and cell charging voltage. Therefore, having a lower LFO content and avoiding higher-voltage cell charging would lead to less oxygen release as 75% of the oxygen is released when the OCP of LFO reaches the second voltage plateau (~4.0 V). However, oxygen release and its precise effect on cell degradation is worthy of further investigation and would be part of our future work.

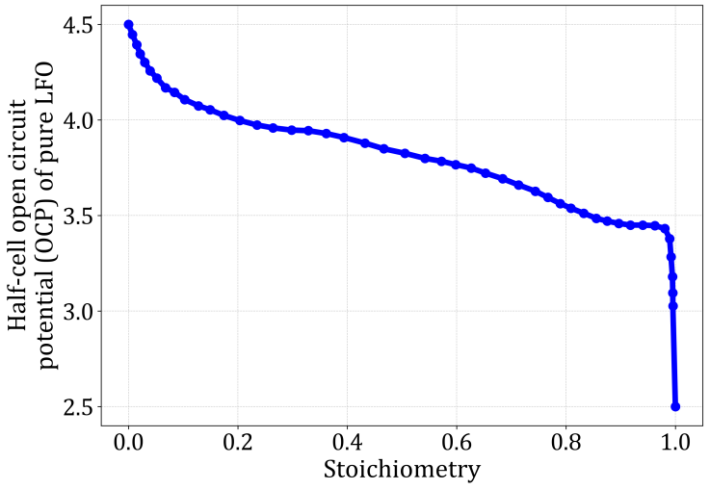

Figure 1: Half-cell open circuit potential (OCP) of a pure LFO material vs stoichiometry (Liu et al., 2024, Sepideh, 2017)

Relating composite LFP-LFO cell charging voltage to lithium and oxygen release from LFO and pure LFP cell operating window

Crucially, the useable voltage range for LFP cells is below 3.5V, with the plateau for normal operation being between 3.2-3.4 V depending on stoichiometry and hysteresis. Even accounting for overpotentials during operation it is possible to keep the normal operating window for an LFP full cell below 3.5 V. This means that the release of lithium and oxygen from LFO in a composite LFP/LFO positive electrode (PE) based cells can be fully controlled as it requires the cell to be operated outside LFP's normal operating window by charging so that the composite PE potential rises above 3.5 V. As lithium is released, the necessary potential to release further increases monotonically.

Exploring lithium release from LFO through PyBaMM model

To understand the effect of releasing lithium from LFO we created a physics-based model in an open-source battery modelling environment PyBaMM to explore the usage of LFO in commercial LFP cells. We carefully parameterized it to be representative of a large commercial cell. The model was then adapted to include a composite PE by including an additional set of equations and the OCP curve of LFO which would be solved in parallel with the LFP equations. A description of the equations, parameters, and other information necessary is included in part 1 of the methods section. The model was thermally lumped, but for this study, which was to be the first to explore the effect of LFO additives in a full-cell model, reproducing thermal gradients and inhomogeneities within a cell was not considered a priority.

In the simulations we included a reference performance test (RPT) every 25 charge-discharge aging cycles, which is common during experimental studies, to demonstrate the effect of LFO additives on degradation in a familiar way. Before each RPT, a controlled lithium release charging event was performed. During our baseline lithium release charging event, the cell is overcharged until the cell voltage reaches 4.5 V, and then the cell is rested for 1 minute. Although this represents an extreme lithium and oxygen release event, and it is possible to release them in a more controlled way by overcharging to lower voltages and/or for shorter times, this is similar to how LFO has been used and studied in most academic research (Johnson et al., 2010), (Su et al., 2016), (Liu et al., 2024). We first designed and explored four lithium release control methods based on different patterns of controlled lithium release charging events to investigate the impact of lithium release speed (fast or slow) and timing (early or later part of cell life) on cell life, which we have named Case 1 through to Case 4. We then designed a non-conventional lithium release control method based on coulomb counting controlled charging events (fixed capacity charging) which we named Case 5. As described previously, for each case, the simulation included the set of 25 charge-discharge aging cycles, followed by a controlled lithium release event (which is either a normal charging, an overcharging, or a coulomb counted controlled charging cycle) and a reference performance test (RPT), repeated over 80 times to get 2000 charge/discharge aging cycles. Detailed information on all the cases can be found in part 3 of the methods section.

Figures 2 and 3 show the results from Case 1 in a commercial cell with 4% (by weight) LFO content. Case 1 has a controlled lithium release overcharging event before each RPT but, for simplicity, both figures only show the first six of these events because nearly all the lithium was released from LFO. An initial guess of 4% LFO was made, which could theoretically release enough lithium to

compensate for ~16% of lost lithium inventory (as each mole of LFO theoretically releases 4 moles of lithium). Also, low LFO content ensures that less oxygen is released thereby avoiding oxygen-triggered degradation.

Figure 2 shows that during the first 25 normal charging-discharging aging cycles, some lithium was released from the LFO because the normal charging was up to 3.6V and hence some LFO capacity was accessed. However, after the first overcharging event the remaining lithium in the LFO dropped by almost half, releasing a significant amount of lithium into the cell. The consequence of this on the cell balancing can be seen in the positive electrode open-circuit potential which increases significantly. Assuming the cell balancing was optimal at the beginning of life this is not good, essentially the cell has become unbalanced by too much lithium being released too soon. The consequence of this is explored in the next section (Figure 3). After the first overcharge, there is no lithium left in the LFO accessible below 3.6 V, so no further release occurs during normal cycling, and the lithium release from subsequent overcharge events decreases significantly each time.

Most previous academic research (Johnson et al., 2010), (Su et al., 2016), (Liu et al., 2024) has explored the use of lithium inventory as a sacrificial agent either in one go (i.e. all lithium released during the first overcharge itself) or in the first few charge-discharge cycles. Here we will show that the lithium release from additives can be more controlled and gradual, and we will explain the benefits of doing so in greater detail in the next sections.

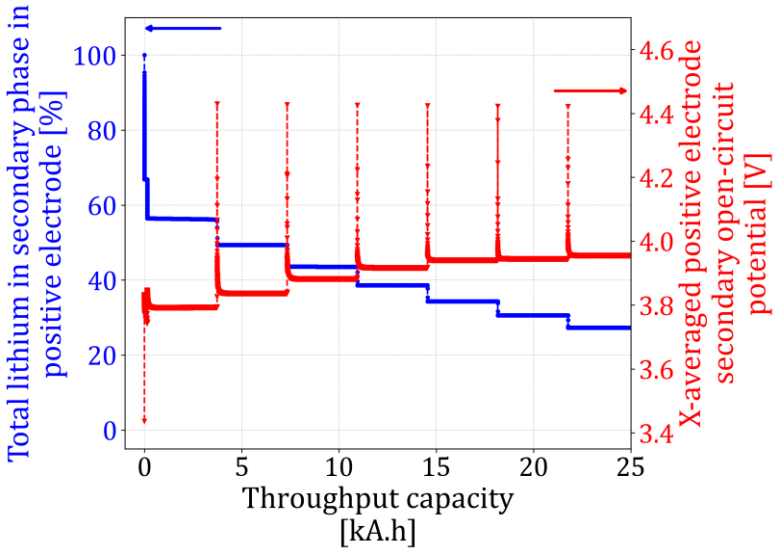

Figure 2: Simulation to show how lithium release & stoichiometric drift from LFO is connected to its OCP & OCP drift respectively.

Consequences of Lithium release from LFO on SEI growth, dead lithium plating, and cell usable capacity

When releasing lithium from LFO it can have both a positive and a negative impact on cell performance and stability. In Case 1, the lithium is released fast and early, at a rate faster than lithium is lost due to the side reactions. This disturbs the cell balancing as the electrodes are forced to host this extra lithium inventory leading to their over-lithiation as shown in Figures 3(a) and 3(e). This causes the OCP of the NE to shift to lower potentials at the end of the charge, pushing it further close to zero and decreasing the reaction overpotentials, as shown in Figures 3(b) and 3 (c). This accelerates the side reactions for SEI layer growth and dead lithium plating (Sulzer et al., 2021), (MARQUIS, 2020), (O'Kane et al., 2022), leading to faster degradation and faster loss of lithium

inventory. Therefore, if lithium is released from the LFO it accelerates the precise problem it is there to mitigate. However, it is not all bad, the amount of lithium lost due to the accelerated side reactions does take time to equal the amount released and temporarily leads to a higher useable capacity whilst the cyclable lithium capacity remains above the beginning-of-life value. As shown in Figure 3(d), at around 25 kAh throughput ~0.175 moles have been consumed by side reactions whilst ~0.25 moles were released from the LFO, leading to a higher useable capacity as shown in Figure 3(f).

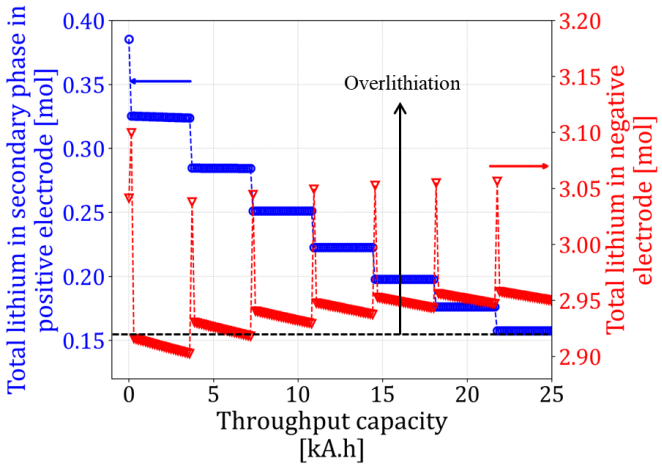

(a)

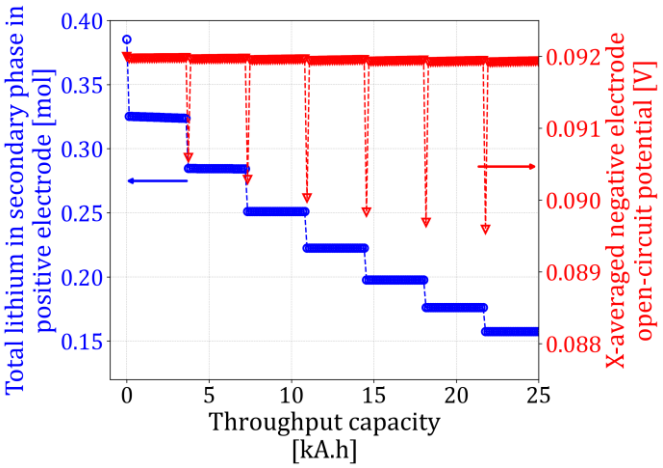

(b)

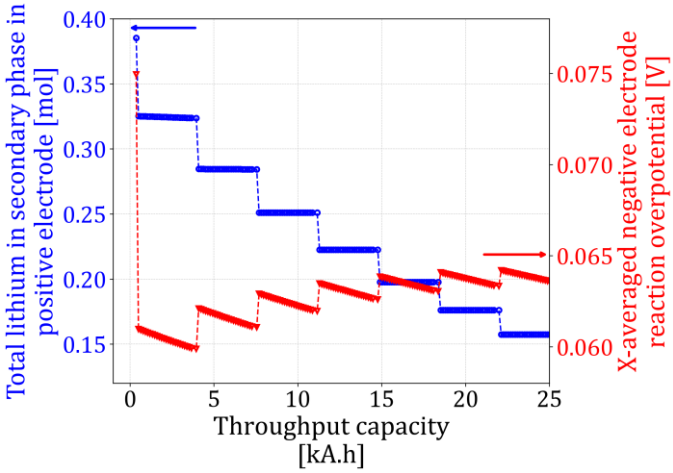

(c)

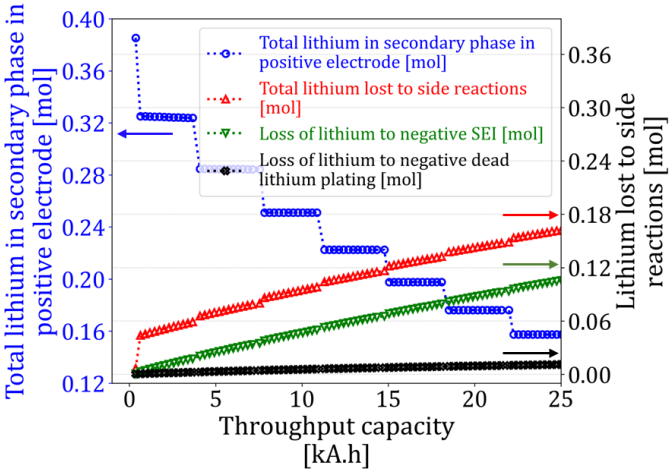

(d)

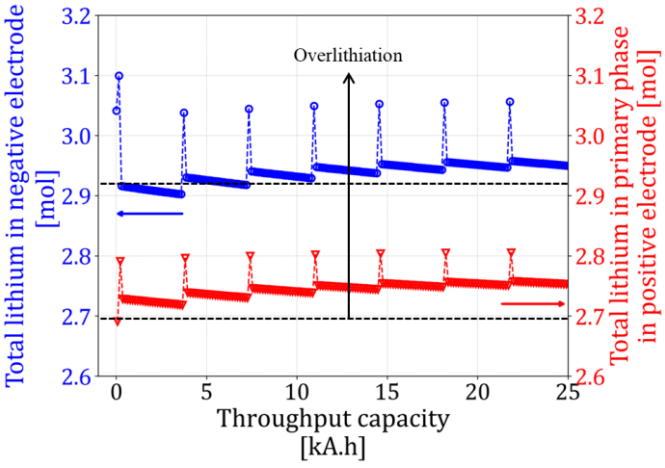

(e)

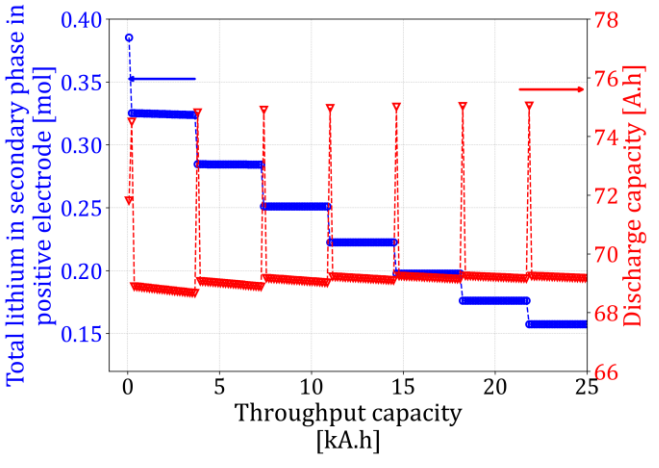

(f)

Figure 3:
(a) 'Total lithium in the secondary phase in PE [mol]' and 'Total lithium in negative electrode [mol]' vs 'Throughput capacity [kA.h]'
(b) 'Total lithium in the secondary phase in PE [mol]' and ' X-averaged negative electrode open-circuit potential [V]' vs 'Throughput capacity [kA.h]'
(c) 'Total lithium in the secondary phase in PE [mol]' and 'X-averaged negative electrode reaction overpotential [V]' vs 'Throughput capacity [kA.h]'
(d) 'Total lithium in the secondary phase in PE [mol]','Total lithium lost to side reactions [mol]', 'Loss of lithium to negative SEI [mol]' and 'Loss of lithium to negative dead lithium plating [mol]' vs 'Throughput capacity [kA.h]'
(e) 'Total lithium in negative electrode [mol]', and 'Total lithium in primary phase in positive electrode [mol]'
(f) 'Total lithium in the secondary phase in PE [mol]', and 'Discharge capacity [Ah]' vs 'Throughput capacity [kA.h]'

From the above analysis, it is clear that releasing too much lithium, although temporarily beneficial in terms of useable capacity, leads to faster degradation and therefore potentially reduced lifetime, not extended lifetime. In the next sections, we show that the key to achieving longer lifetimes may lie in controlling the lithium and oxygen release from LFO more carefully to either delay the release to avoid overlithiation from start or match the release with lithium lost due to side reactions without unbalancing the cell and accelerating the side reactions.

Lithium release control methods and their effect on cell performance

With the help of Case 1, we showed how fast and early lithium release from LFO can impact cells negatively. We now investigate four additional patterns/methods (Case 2 to Case 5) of lithium release in a cell with 4% LFO content and their impact on cell performance. The cell performance was compared by studying how the discharge capacity and cell degradation indicators such as loss of lithium inventory, SEI, lithium plating, and NE porosity evolve with cell capacity throughput. For simplicity, only figures related to the comparison of Case 1, Case 4, and Case 5 are shown here, the Figure for the comparison of Case 1 to Case 3 and all 5 Cases can be found in the Supplementary Section after the references (see Supplementary Figures 1 and 2).
Like Case 1, Cases 2 to 4 show that whenever the overcharge events occur, the release of lithium from LFO happens rapidly (Figure 4(a)), leading to increased rated (RPT) discharge capacity (Figure 4(b)) as well as increased total lithium loss towards the side reactions (increased SEI growth and dead lithium plating) (Figures 4(c) to 4(e)). The formation of SEI and plating causes the porosity of the negative electrode to clog; hence, Figure 4(f) shows the decreasing trend for negative electrode porosity. Case 1 offers higher discharge capacities because of early and fast/frequent lithium release but significantly accelerates cell degradation and porosity clogging. Case 2 delays the lithium release and hence, can provide higher discharge capacities in the later part of cell life. Case 3, due to just 3 overcharge events, could preserve most of the available lithium inventory from LFO resulting in relatively slower cell degradation and less discharge capacities. This is because the cell remains balanced due to less lithium released from LFO. Case 4 offered a better trade-off between the degradation rates and discharge capacities due to the periodic nature of lithium release and its ability to provide enough time for the cell to degrade and achieve a relatively balanced state before the freshly released lithium from LFO starts to overlithiate and unbalance the cell again.
Case 5 works slightly differently from other cases. Here the cell is overcharged until the usable capacity of the cell matches its beginning-of-life value or the charging voltage hits the maximum

cutoff value of 4.5 V- whichever is reached earlier. This contrasts with other cases where every overcharge event has a charge voltage cutoff limit of 4.5 V. Case 5 ensures that the released lithium moles from LFO match with and do not overcompensate for lithium lost to the side reactions. This leads to a more balanced and gradual drop in lithium moles from LFO (Figure 4(a)), almost constant rated discharge capacity (Figure 4(b)), medium degradation rates, and porosity clogging (Figure 4(d) to 4(f)). Once lithium moles from LFO get depleted or are not enough to compensate for lost lithium due to side reactions, a sudden drop in discharge capacity is observed.

It is worth noting that the maximum charging voltage during the controlled lithium release event in Case 5 is not always 4.5 V as the charging is done until the cell capacity equal to BOL capacity is achieved (i.e. fixed capacity charging). As a result, the average OCP of LFO doesn't achieve high voltage values until way later in cell life (Supplementary Figure 3). Since the cell operates way below 4.5 V PE OCP, the oxygen release would happen gradually and at a sufficiently controlled rate, allowing cathode coating agents to effectively scavenge it. Because of lower operational PE OCP, Case 5 is expected to perform even better when the charging events are followed by the CV phase compared to Case 1 and Case 4 because holding the cell at high charging voltages (or high PE OCP) would accelerate oxygen evolution. For this reason, Case 1 and Case 4 would need more careful consideration while implementing them in real systems.

These findings suggest that the choice of control adopted for lithium and oxygen release can significantly alter cell performance. Hence, based on the real-life use case and cell performance expectations, suitable control algorithms must be designed and implemented to tailor the timing and speed of lithium release.

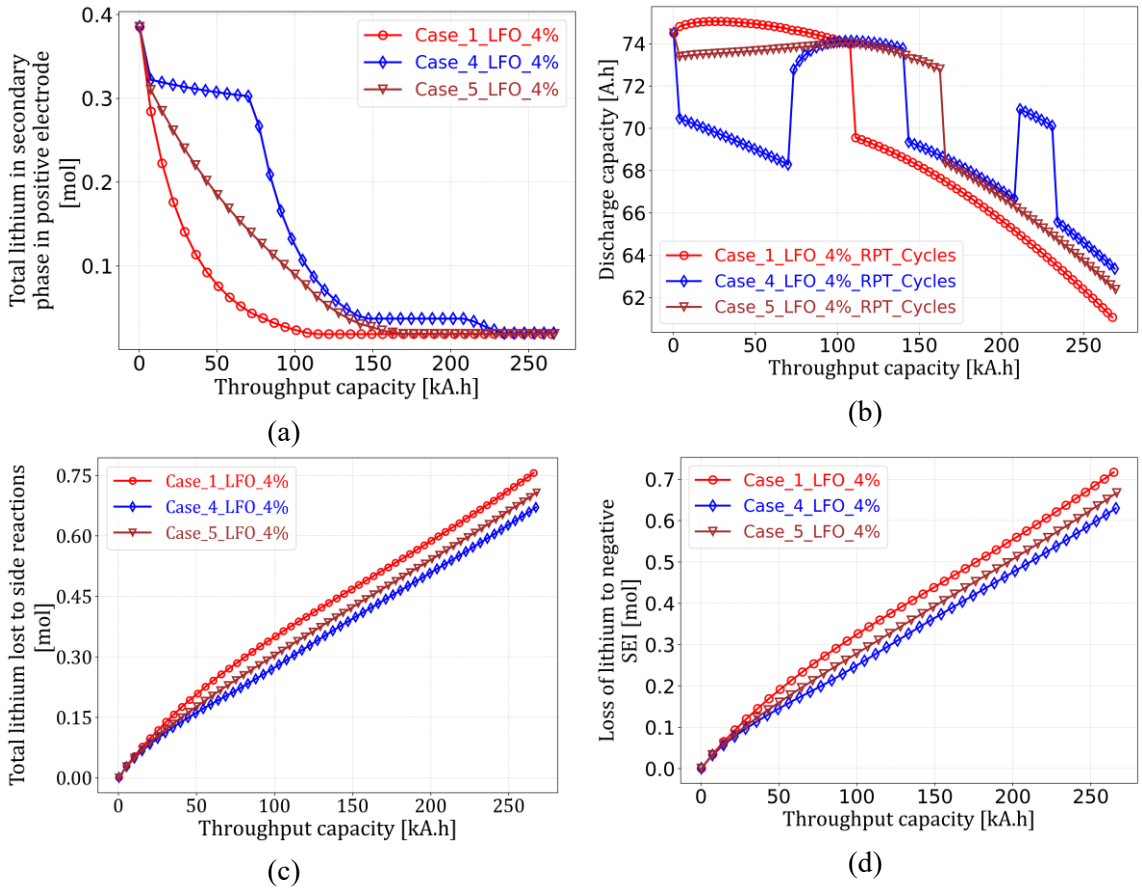

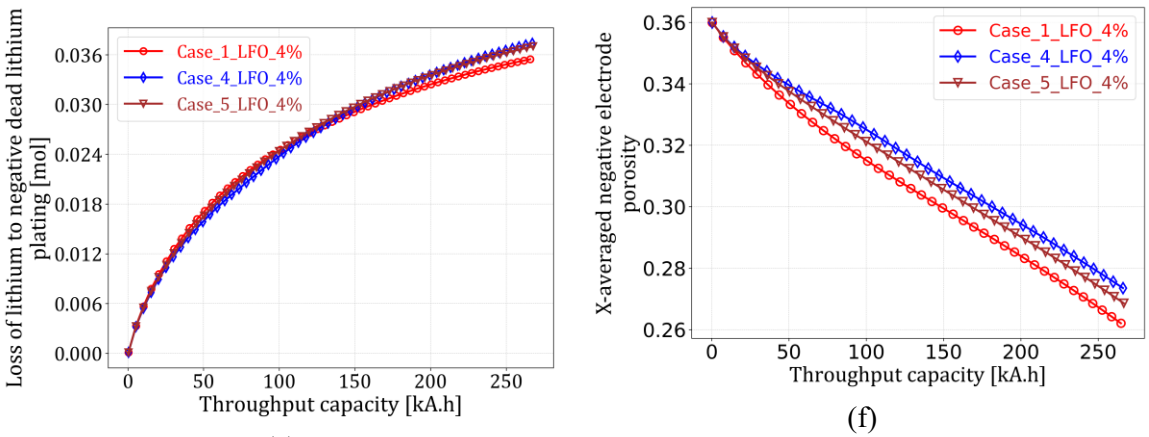

(e) (f)

Figure 4: Comparison of Case 1, Case 4, and Case 5 against (a) lithium release from secondary phase i.e. LFO (b) RPT cycles discharge capacity (rated capacity) (c) Total lithium lost to side reactions (d) the loss of lithium to negative SEI (e) the loss of lithium to negative dead lithium plating, and (f) the average NE porosity (spatially averaged in the x-direction)in LFP-LFO composite cell

Effect of LFO weight fraction on cell performance

In the previous section, Case 4 & Case 5 were shown to have relatively better performance compared to other cases at a 4% LFO fraction. We now choose Case 5 to explore the effect of 1% and 10% LFO weight fractions on cell performance and compare it with the previously discussed case of 4% LFO.

For the 1% LFO, the initial available lithium inventory is low (Figure 5(a)), and as the cell degrades, the lithium from LFO gets depleted early in cell life. Therefore 1% LFO was not able to provide sustained rated discharge capacity for long and capacity started to drop linearly after around 60 kAh throughput capacity (Figure 5(b)). Also, the total degradation rates for side reactions (SEI and dead lithium plating) and NE porosity clogging were comparatively lower than the 4% LFO fraction (Figure 5(c) and 5(d)). This is again because of fewer available lithium moles from LFO, and their early consumption was not able to disturb the cell balancing for long.

Increasing the LFO weight fraction to 10% increased the rated discharge capacity initially because more lithium inventory/cyclable lithium is available for access from LFO (Figure 5(a) and 5(b)), however, the benefit is temporary, and a steep drop in rated discharge capacities is observed later in cell life (Figure 5(b)). Also, excessive availability of lithium inventory from LFO for longer periods keeps the cell in a highly unbalanced and unstable state for longer, leading to accelerated side reactions (Figure 5(c)) and NE porosity clogging (Figure 5(d)). This leads to cell failure when NE gets clogged completely (zero porosity).

These findings reveal a clear trade-off between discharge capacity and long-term cell performance for a chosen LFO fraction. As discussed previously, although the oxygen release in Case 5 is expected to be balanced, a higher fraction of LFO would lead to excess oxygen evolution whose effect on degradation may not be ignored. Hence one must carefully choose the optimal weight fraction of LFO by looking at the desired cell performance over time.

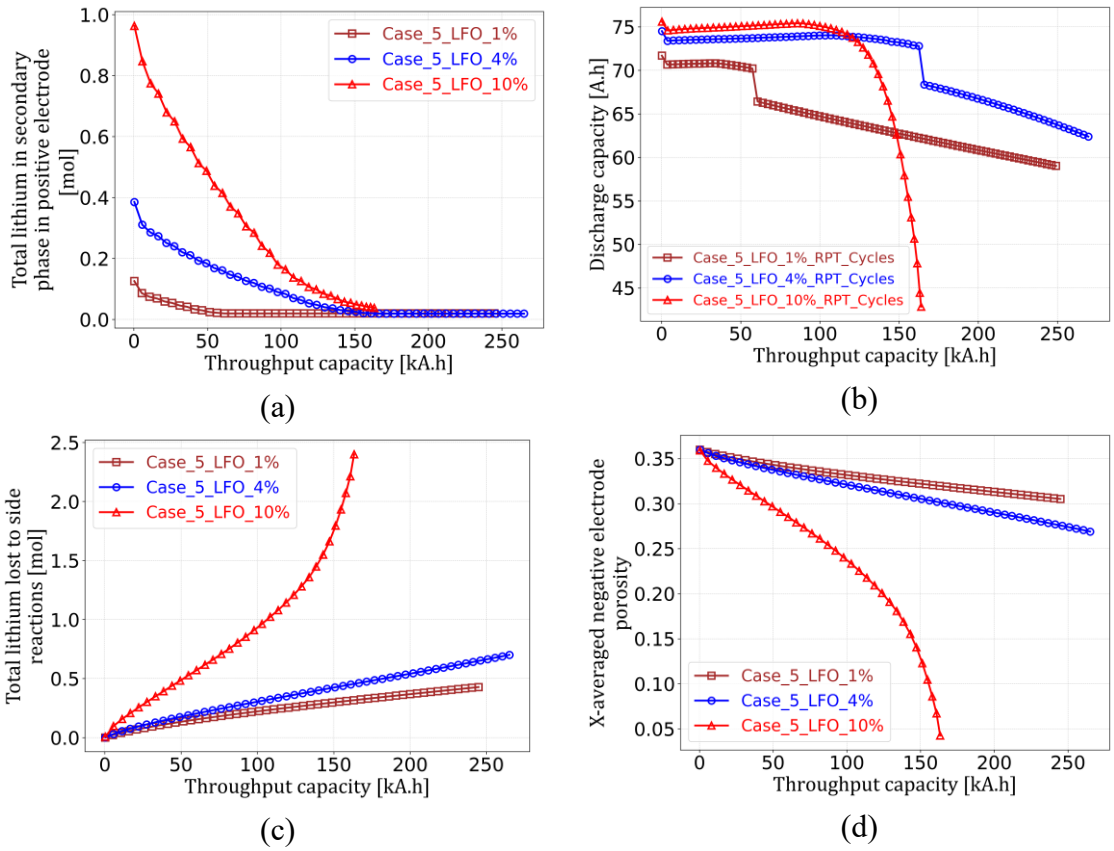

Figure 5: Comparison of 1%, 4% & 10% LFO weight fraction for Case 5 (a) lithium release from secondary phase i.e. LFO (b) RPT cycles discharge capacity (rated capacity) (c) total lithium lost to side reaction (SEI + Dead lithium plating), and (d) the average NE porosity (spatially averaged in the x-direction) in LFP-LFO composite cell.

Overdesigning the cell to avoid cell unbalancing due to NE overlithiation

Model results in previous sections revealed that for a perfectly balanced cell, even with optimal LFO content (e.g. 4% LFO), lithium release from LFO is sufficient to overlithiate the electrodes leading to causing the unbalanced cell and accelerated degradation. We explored the possible control methods to better manage cell overlithiation and degradation but it may not be fully avoided. In certain scenarios, cell designers or process engineers must perform frequent controlled lithium release events (like Case 1) so that oxygen can be released and degassed very early in cell life (preferably during formation). The controlled lithium release events would lead to cell overlithiation. With the above scenario in mind and to better control cell overlithiation, we overdesiged a cell using PyBaMM simulation. The cell overdesign was done by using a slightly larger NE than the perfectly balanced cell. The NE thickness was carefully increased such that the NE to primary PE capacity ratio (NP capacity ratio) of 1.25 is achieved (higher NE overhang) compared to the 1.1 base case NP capacity ratio. We refer to this overdesign as the “Cheesecake with just extra cheese!” especially because the other fundamental physical properties of NE such as surface concentrations, porosity, and particle sizes were kept unchanged. To compare the degradation performance of overdesigned cells, the BOL cell performance was matched by adjusting the initial stoichiometries of NE and PE.

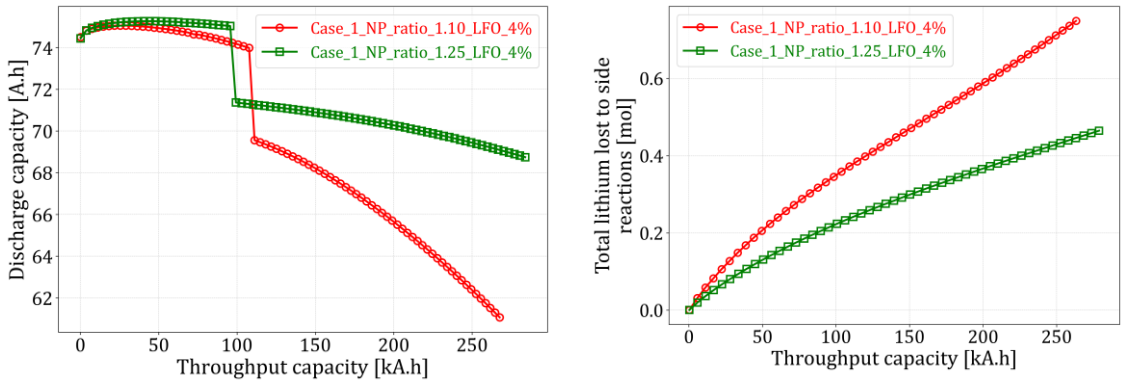

(a) (b)

Figure 6: Comparison of Cell with NP ratio of 1.1 (red, round marker) vs NP ratio of 1.25 (green, square marker) for 4% LFO weight fraction for Case 1 (a) RPT cycles discharge capacity (rated capacity) and (b) total lithium lost to side reaction (SEI + Dead lithium plating)

Figure 6 above compares the Case 1 performance for the base case NP ratio of 1.1 and the overdesigned NP ratio of 1.25 for 4% LFO content. The discharge capacity in Figure 6(a) was observed to be much higher for the overdesigned cell as overdesigning of the cell minimizes overlithiation and cell degradation rates leading to lesser lithium loss to the side reactions as shown in Figure 6(b).

Clearly, the overdesigning of the cell can benefit its longevity immensely, however, it is worth noticing that a larger NE overhang would lead to lower cell energy density. Therefore, it is important to study the trade-off between the longer cell life and cell energy density in the future. Also, the NP ratio of 1.25 was chosen just to show the proof of concept and further study would be needed to find the optimal NP ratio corresponding to each of the five Cases and various LFO fractions discussed previously.

Conclusions

We developed a composite cathode (LFP-LFO) based full-cell physics-based model coupled with multiple degradation mechanisms in PyBaMM, which is the first to demonstrate how LFO can be employed in large commercial LFP cells. Cell performance was measured by studying the variation of discharge capacities, SEI formation, lithium plating, and porosity clogging on NE. Model results demonstrated that maintaining the cell balancing is the key to achieving longer life "zero-degradation" batteries. We explored methods to control the speed and timing of lithium release. We demonstrated that cell balancing can be maintained by slow controlled release of lithium calibrated to match the rate of lithium lost and also by overdesigning the cell. The lower to medium LFO fraction such as 4% along with a suitable lithium release control method could be critical to managing oxygen release and the associated cell degradation, however, this required further investigation. We also conclude that a higher LFO fraction in the cell might not be beneficial for long-term cell performance.

The results and conclusions from this work will be of direct relevance to cell designers and battery control engineers. Also, the model framework developed in this work can easily be adapted to other composite chemistries, such as LFP-LMFP and composite nickel-based chemistries. Therefore,

could be of great importance to researchers in academia as well as industry to study and design new high-performance composite electrode cells.

Methods

Part1: PyBaMM Model setup & model assumption

The standard Doyle-Fuller-Newman (DFN) model was set up in PyBaMM using the model options highlighted in Figure 7. The details about all the model options can be found in the PyBaMM documentation (PyBaMM, 2024). To ensure simplicity while maintaining the model as a close representative of actual LFP-LFO cell behaviour and not to deviate from the primary goal of showing the proof of concept for designing zero degradation battery, multiple considerations were made in the model. A pure LFP cell model was built and parameterized using (Prada et al., 2013) which then was modified to consider degradation mechanisms such as SEI formation, lithium plating, conversion of plated lithium to dead lithium, and the resulting porosity clogging at NE. The degradation parameters were considered as per (O'Kane et al., 2022). NE was considered to have just graphite and hence the single phase whereas two phases were implemented for composite PE with LFP as the primary phase and LFO as the secondary phase. Charge transfer kinetics for NE and PE primary phase (LFP) were modelled using Butler-Volmer kinetics whereas Tafel kinetics works best for LFO as it can only release lithium (de-intercalated) due to its lithium scarifying nature. Hysteresis in LFP was accounted for by considering the current sigmoid model for the primary phase.

```
model_options = {
        SEI": ("interstitial-diffusion limited", "none"),
        "lithium plating": "partially reversible",
        "lithium plating porosity change": "true",
        "open-circuit potential": (("current sigmoid", "current sigmoid"), ("current sigmoid", "current sigmoid")),
        "SEI porosity change": "true",
        "intercalation kinetics": (("symmetric Butler-Volmer", "symmetric Butler-Volmer"), ("symmetric Butler-Volmer", "Tafel")),
        "particle phases": ("1", "2"),
    }
```

Figure 7: Snapshot of model options considered for setting the PyBaMM model

As the work was primarily aimed at demonstrating and explaining the science behind employing LFO by building a cell model that closely mimics the characteristics of real-life commercial LFP cells, hence, the work does not focus on a) experimental validation, b) the effect of temperature., thermal gradients and inhomogeneities on cell degradation, c) performing sensitivity analysis on various degradation-related parameters. Some of the above-listed work forms part of our future work.

Part2: Setting up a virtual experiment in PyBaMM

The virtual experiments were designed to simulate the long-term aging of a full LFP-LFO cell (Figure 8) which undergoes multiple constant-current (CC) charges, rests,constant current (CC) discharges and rests.

The virtual experiment is designed to perform the one-breaking cycle followed by multiple repetitions of aging cycles and characterization reference performance tests (RPTs). The virtual test

starts with one breaking cycle involving charging, followed by discharge and rest, and then charging again. After that, the first reference performance test (RPT0) was done to measure BoL-rated discharge capacity and then the aging cycles were performed. Aging cycles consist of a set of 25 cycles of CC charge-rest (1 min)-CC discharge-rest (1 min) steps (represented by the constant 'N' in Figure 8). This set of 25 Aging cycles is followed by one controlled lithium release charging event i.e. CC charge-rest(1 min) and a reference performance test (RPT). Depending upon the control methods/cases adopted, (a discussion on which can be found in Part 3 of the methods section, for lithium release from LFO) the controlled lithium release charge event could either be a normal charge, an overcharge, or coulomb counted controlled charging (fixed capacity charging). The set of 25 aging cycles, one controlled lithium release charging event, and a characterization RPT is then repeated 80 times to achieve 2000 aging cycles ('80' repetitions are represented by the constant 'M' in Figure 8). Discharge capacity obtained from discharges done during aging cycles was categorized as usable discharge capacity or aging cycles discharge capacity whereas discharge capacity obtained from RPT0 and the '80' other RPTs are collectively referred to as RPT cycles discharge capacity.
The charge & discharge rates considered for aging cycles and breaking cycles were fixed at 0.5C whereas the discharge rate for characterization RPTs was considered 0.2C. For normal charging, lower and upper cutoff voltage limits were 2.5 V, and 3.6 V respectively For overcharging voltage limits considered were 2.5 V and 4.5 V respectively. The upper cutoff voltages were followed by a 1-minute rest.

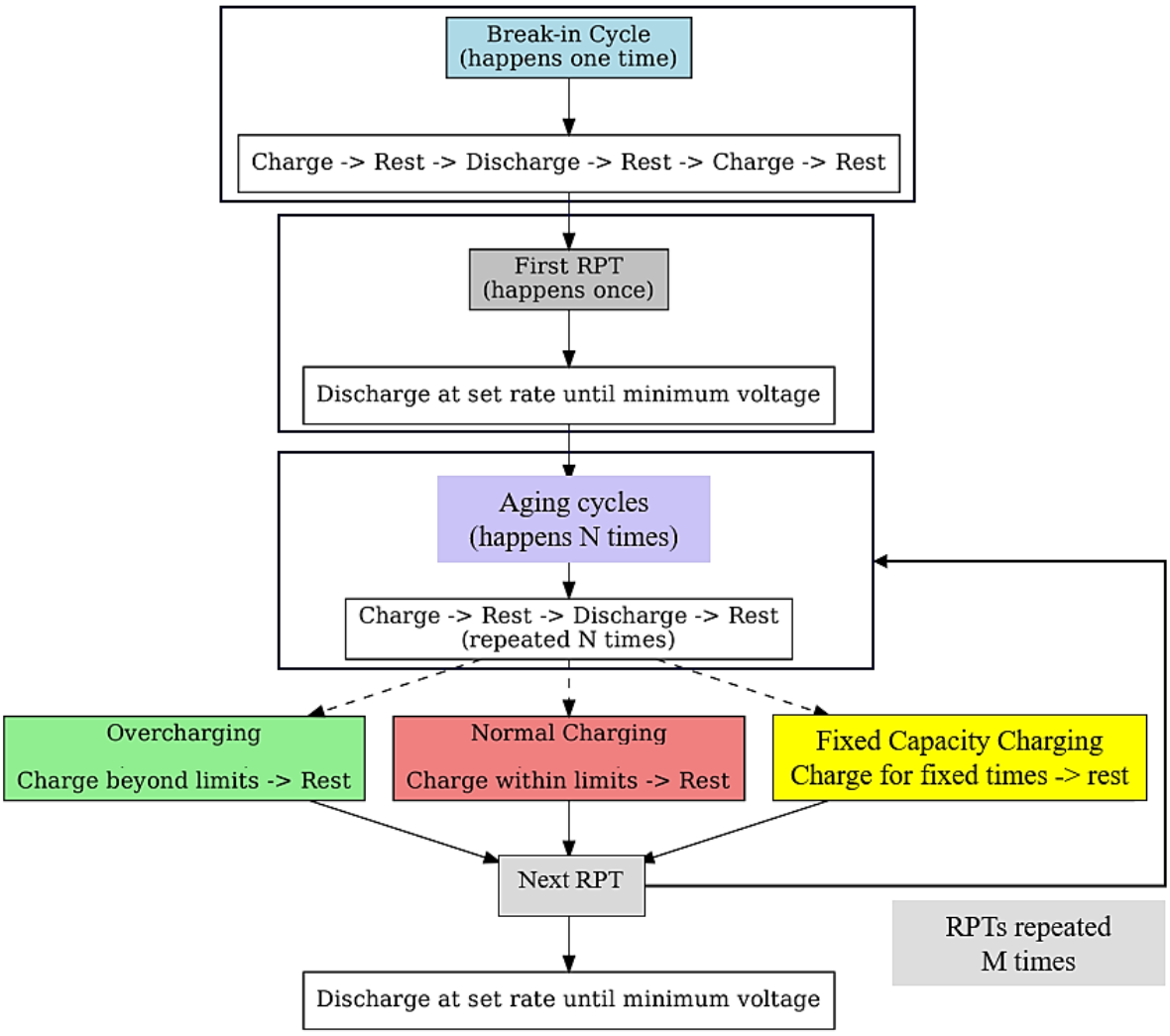

Figure 8: Snapshot of virtual experiment considered in the PyBaMM model

Part3: Setting up lithium release patterns (cases) in PyBaMM

We designed five controlled methods/lithium release patterns/cases. These cases are essentially designed to control the speed (fast or slow) and timing (early or later part of cell life) of lithium release from LFO. Case 1 represents the early, fast, and frequent lithium release from LFO where overcharges are done before every RPT with a total of 80 overcharges. Case 2 illustrates fast and frequent lithium release but starting later after cell throughput capacity equivalent to 1000 aging cycles is achieved. Here, overcharge is done starting from the 40th RPT (i.e. delayed lithium release from LFO) and continuously until the 80th RPT with a total of 40 overcharges. Case 3 represents slow and infrequent lithium release where overcharge is done before the 20th, 40st, 60^{st,} and 80th RPTs with only 4 overcharges. Case 4 represents the case of fast and frequent but intermittent lithium release where overcharges are done continuously between the 20th to 40th RPT and then the 60th to 80th RPT with a total of 40 overcharges. Case 5 performs coulomb counted controlled charging i.e. fixed capacity charging meaning cell is made to charge until it achieves BoL usable discharge capacity, or it hits the upper cutoff voltage safety limit of 4.5 V. This represents the case where we are indirectly calibrating lithium release to match the lithium lost towards side reactions and hence avoiding overlithiation of NE.

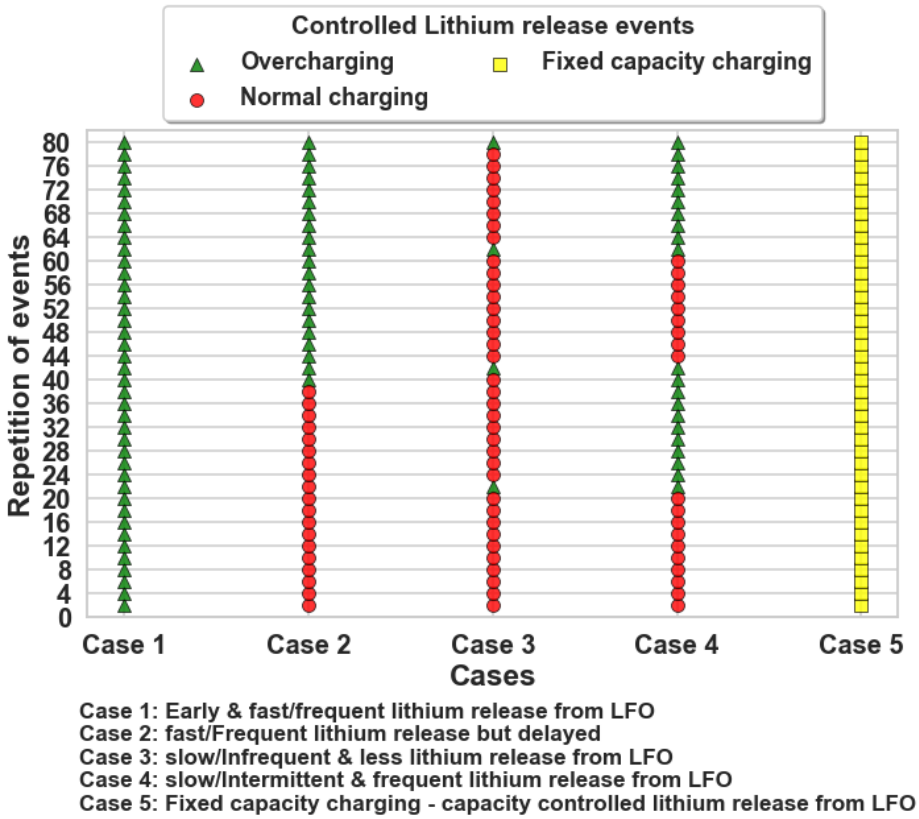

Figure 9: Snapshot of a number of lithium release controlled charging events just before characterization RPTs. The green triangle at a particular characterization RPT number represents that overcharging is done just before that characterization RPT, Red dot at a particular characterization RPT number represents just the normal charging is done before that characterization RPT and the Yellow square at a particular characterization RPT number represents a coulomb counted (fixed capacity) charging events just before that characterization RPT.

References

[1] BIRKL, C. R., ROBERTS, M. R., MCTURK, E., BRUCE, P. G. & HOWEY, D. A. 2017. Degradation diagnostics for lithium ion cells. *Journal of Power Sources,* 341**,** 373-386.

[2] DOSE, W. M., MARONI, V. A., PIERNAS-MUÑOZ, M. J., TRASK, S. E., BLOOM, I. & JOHNSON, C. S. 2018. Assessment of Li-Inventory in Cycled Si-Graphite Anodes Using LiFePO4as a Diagnostic Cathode. *Journal of The Electrochemical Society,* 165**,** A2389-A2396.

[3] EDGE, J. S., O'KANE, S., PROSSER, R., KIRKALDY, N. D., PATEL, A. N., HALES, A., GHOSH, A., AI, W., CHEN, J., YANG, J., LI, S., PANG, M. C., BRAVO DIAZ, L., TOMASZEWSKA, A., MARZOOK, M. W., RADHAKRISHNAN, K. N., WANG, H., PATEL, Y., WU, B. & OFFER, G. J. 2021. Lithium ion battery degradation: what you need to know. *Phys Chem Chem Phys,* 23**,** 8200-8221.

[4] JOHNSON, C. S., KANG, S. H., VAUGHEY, J. T., POL, S. V., BALASUBRAMANIAN, M. & THACKERAY, M. M. 2010. Li2O Removal from Li5FeO4: A Cathode Precursor for Lithium-Ion Batteries. *Chemistry of Materials,* 22**,** 1263-1270.

[5] LIU, X., LIU, J., PENG, J., CAO, S., HU, H., CHEN, J., LEI, Y., TANG, Y. & WANG, X. 2024. Addressing the initial lithium loss of lithium ion batteries by introducing pre-lithiation reagent Li5FeO4/C in the cathode side. *Electrochimica Acta,* 481.

[6] MARQUIS, S. G. 2020. *Long-Term Degradation of Lithium-ion Batteries.* Doctor of Philosophy, University of Oxford.

[7] MURRAY, C. 2024. Rimac using pre-lithiation for 'zero capacity fade for first two years' in BESS. *Energy Storage News*.

[8] O'KANE, S. E. J., AI, W., MADABATTULA, G., ALONSO-ALVAREZ, D., TIMMS, R., SULZER, V., EDGE, J. S., WU, B., OFFER, G. J. & MARINESCU, M. 2022. Lithium-ion battery degradation: how to model it. *Physical Chemistry Chemical Physics,* 24**,** 7909-7922.

[9] PATHIRANA, T. 2024. *CATL's SECRET to "Zero" Degradation Batteries: Unveiling the Potential of LFO Cathode Additives* [Online]. Available: https://www.linkedin.com/pulse/catls-secret-zero-degradation-batteries-unveiling-lfo-pathirana-yfsuc/ [Accessed].

[10] PRADA, E., DI DOMENICO, D., CREFF, Y., BERNARD, J., SAUVANT-MOYNOT, V. & HUET, F. 2013. A Simplified Electrochemical and Thermal Aging Model of LiFePO4-Graphite Li-ion Batteries: Power and Capacity Fade Simulations. *Journal of The Electrochemical Society,* 160**,** A616-A628.

[11] PYBAMM. 2024. *PyBaMM documentation* [Online]. Online. Available: https://docs.pybamm.org/en/stable/ [Accessed].

[12] SEPIDEH, A. 2017. *Lithium-Ion battery SOC estimation.* Doctor of Philosophy, University of Waterloo.

[13] SU, X., LIN, C., WANG, X., MARONI, V. A., REN, Y., JOHNSON, C. S. & LU, W. 2016. A new strategy to mitigate the initial capacity loss of lithium ion batteries. *Journal of Power Sources,* 324**,** 150-157.

[14] SULZER, V., MARQUIS, S. G., TIMMS, R., ROBINSON, M. & CHAPMAN, S. J. 2021. Python Battery Mathematical Modelling (PyBaMM). *Journal of Open Research Software,* 9.

Supplementary Section

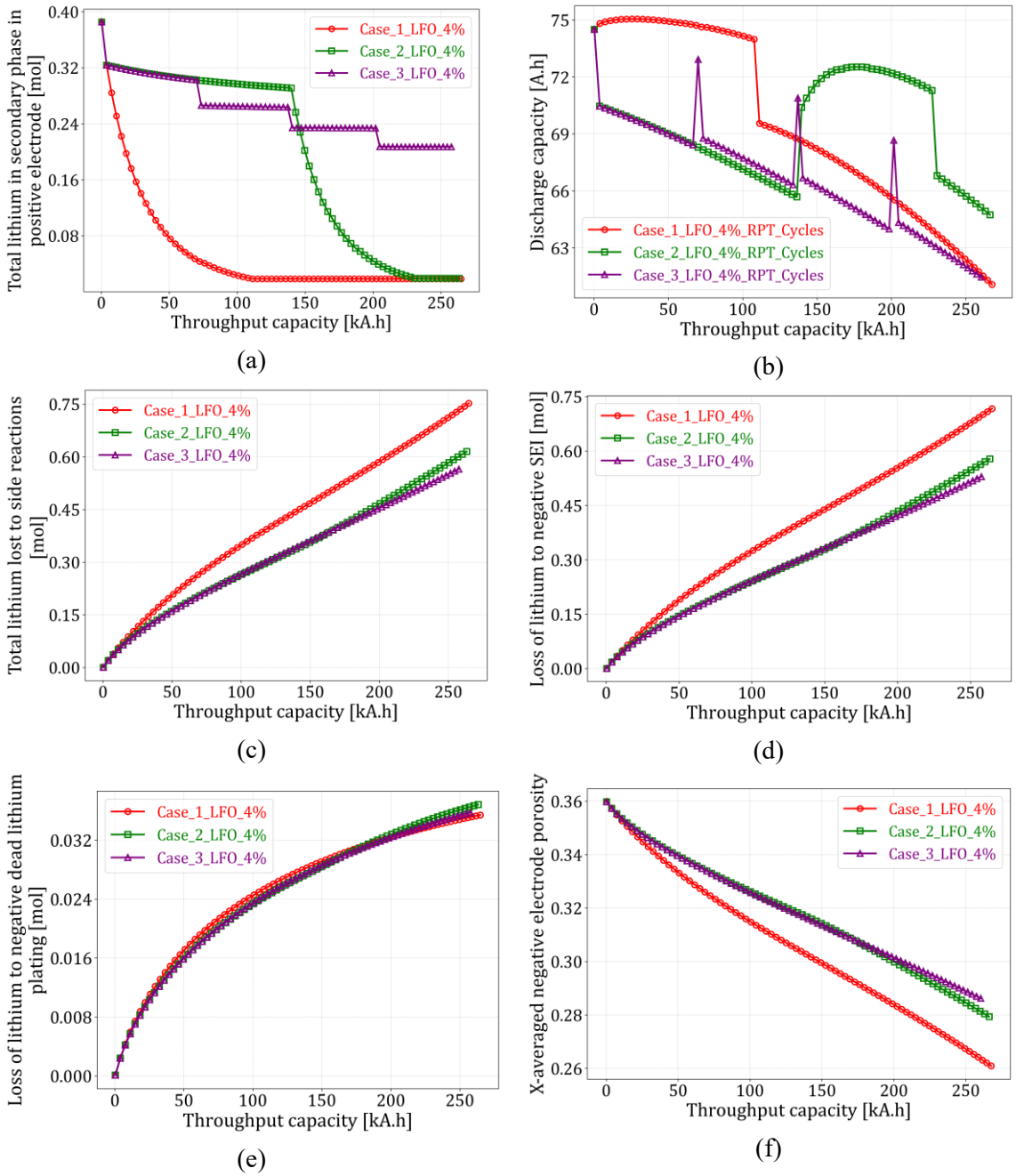

Supplementary Figure 1: Comparison of Case 1, Case 2, and Case 3 against (a) lithium release from secondary phase i.e. LFO (b) RPT cycles discharge capacity (rated capacity) (c) Total lithium lost to side reactions (d) the loss of lithium to negative SEI (e) the loss of lithium to negative dead lithium plating, and (f) the average NE porosity (spatially averaged in the x-direction)in LFP-LFO composite cell

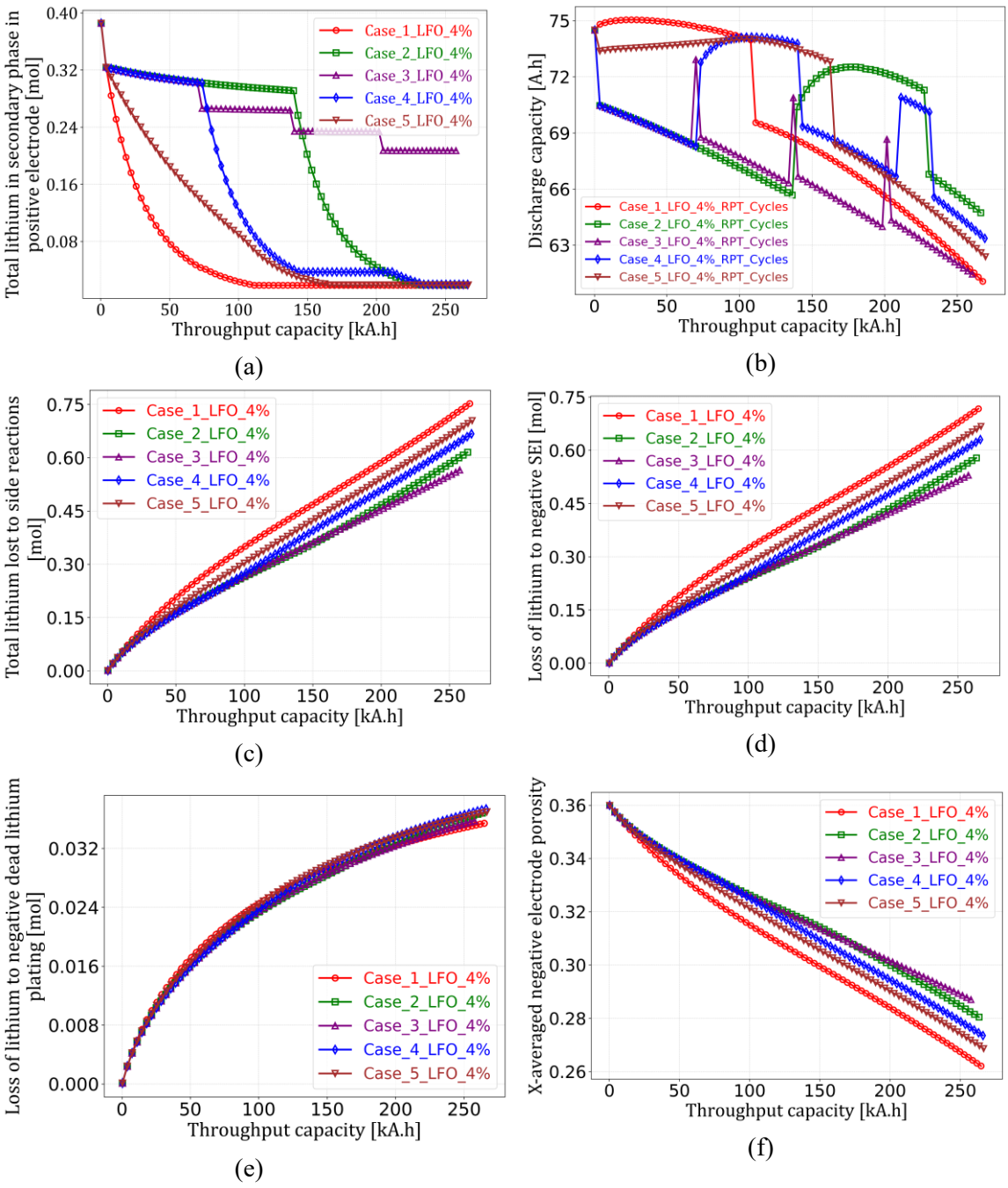

Supplementary Figure 2: Comparison of Case 1, Case 2, Case 3, Case 4, and Case 5 against (a) lithium release from secondary phase i.e. LFO (b) RPT cycles discharge capacity (rated capacity) (c) Total lithium lost to side reactions (d) the loss of lithium to negative SEI (e) the loss of lithium to negative dead lithium plating, and (f) the average NE porosity (spatially averaged in the x-direction)in LFP-LFO composite cell

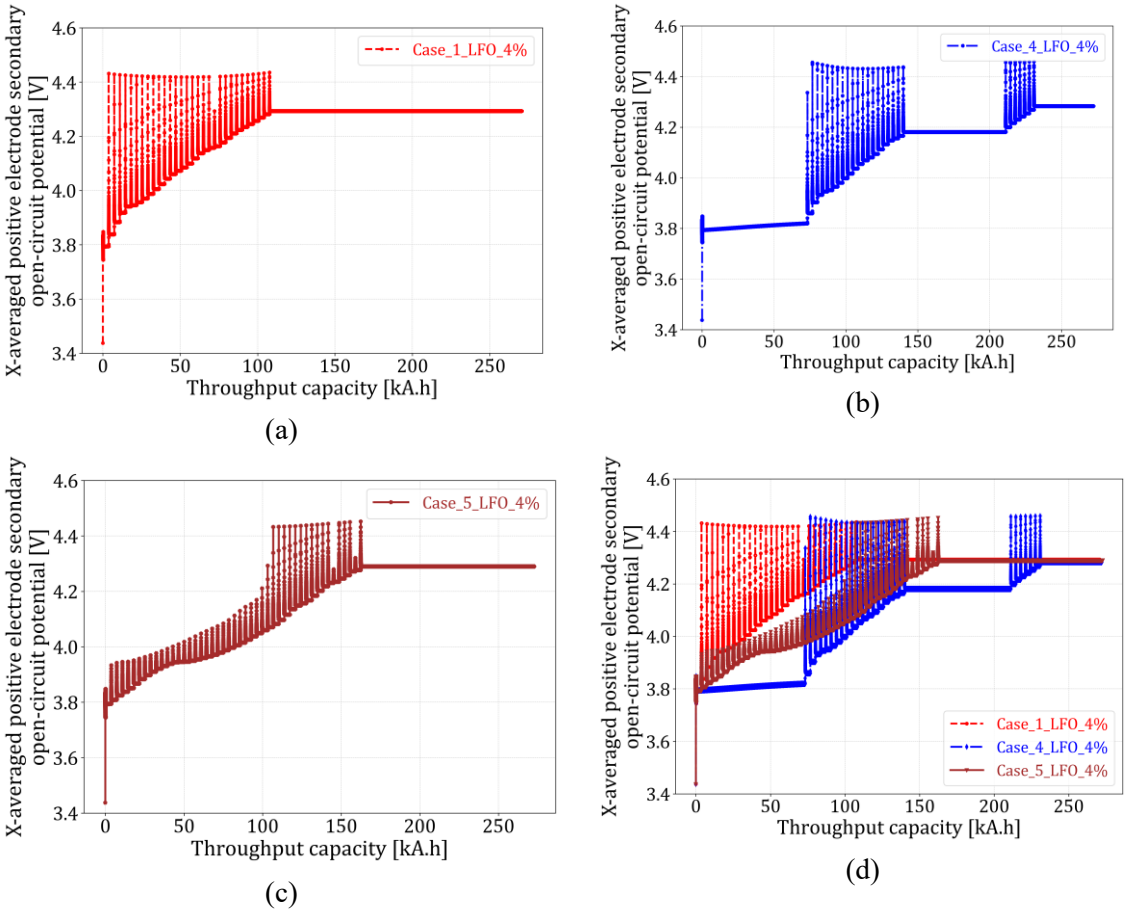

Supplementary Figure 3: X-averaged positive electrode secondary open-circuit potential [V] for (a) Case 1 (b) Case 4 (c) Case 5 (d) comparison of Case 1, Case 4, Case 5